Peptide Coatings **Hot Paper**

International Edition: DOI: 10.1002/anie.201601603
German Edition: DOI: 10.1002/ange.201601603

Easy Access to Functional Patterns on Cellulose Paper by Combining Laser Printing and Material-Specific Peptide Adsorption

*Steffi Große⁺, Patrick Wilke⁺, and Hans G. Börner**

Abstract: *Phage display biopanning is used to identify peptides that show material-selective adsorption, effectively distinguishing between the cellulose of paper and the printed toner of standard office laser printers. These genetically selected 12mer peptides can selectively coat either non-printed cellulose or printed toner patterns. Furthermore, triazolindione ligation chemistry is exploited to introduce, for example, dyes or functional peptides selectively to the coatings. The strategy offers an easy access towards the patterned functionalization of paper-based materials, which potentially is of relevance for low-cost diagnostics or biomedical devices.*

Cellulose is one of the most abundant materials in nature and widely exploited owing to its sustainability, biocompatibility, biodegradability, and low cost.[1] Within the last few decades, cellulose-based materials have attracted a growing interest. For instance, nanocellulose fibrils can strengthen composite materials or form micro-cellulose scaffolds for diagnostic sensors.[2] Moreover, bulk cellulose was used for protective coatings or size-exclusion ultrafiltration membranes.[3] Paper constitutes the most widely available cellulose-derived material and paper-based applications, such as paper microfluidics, electrodes, and sensors are rapidly developing as low-cost devices.[4] Whitesides et al. reported microfluidic analytical devices (μPADs) using paper as the platform.[2c] Recently, Barner-Kowollik et al. applied photopatterning to spatially control the covalent attachment of anti-fouling polymers or peptides on paper.[5] Furthermore, a set of highly effective ligation tools are available, enabling the modification of hydroxy groups on cellulose.[6]

A more straightforward strategy to introduce chemical functions or physical properties in macro and micro patterns on paper could use commercially available printing devices. Standard inkjet printers allow for the precise deposition of down to picolitre volumes onto different supports.[7] This technology platform was utilized for the development of new low-cost materials, including printing of organic electronics, polymer coatings or biomolecules addressing applications from microfluidic systems and sensors to tissue engineering scaffolds.[7,8] Although inkjet printing is promising, the formulation of functional inks suitable for printing still limits the diversity. An alternative approach can circumvent those restrictions by combining top-down and bottom-up processes, fusing laser printing with self-assembly (Figure 1). Thereby, toner patterns printed by office laser printers and non-printed cellulose paper surfaces are selectively recognized and coated with either toner or cellulose binding peptides, respectively.

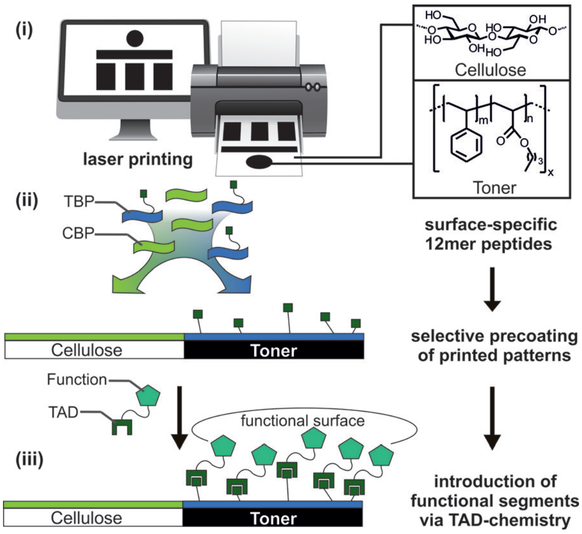

Figure 1. Schematic illustration of the process towards functional patterns. Laser printing of paper is performed by a standard office laser printer (i). A selective coating of printed patterns and non-printed paper regions is achieved by the specific adsorption of peptides on these areas (ii; CBP = cellulose binding peptide; TBP = toner binding peptide). Subsequent functionalization of, for example, toner-binding peptides occurs by regio-selective ligation of functional entities (iii).

Recently, peptides and peptide-polymer conjugates proved to constitute a capable platform to introduce functions to surfaces of various inorganic or organic (nano)particles or sensors.[9] Biocombinatorial means of phage display biopanning reveals peptide sequences, which possess material-specific adsorption. These have been shown to selectively bind onto conducting polymers,[10] to distinguish poly(methacrylate)s with different tacticity,[11] or to recognize single carbon variations among benzene derivatives.[12] Furthermore, peptides could be selected via phage display that predominantly associate onto specific planes of inorganic materials during the crystallization processes of, for example, ZnO,[13] Ag nanoparticles,[14] or Pt nanocrystals.[15] Besides these, peptides that adsorb to octyltrimethoxysilane printed

---

[*] S. Große,[+] Dr. P. Wilke,[+] Prof. H. G. Börner
Humboldt-Universität zu Berlin, Department of Chemistry
Laboratory for Organic Synthesis of Functional Systems
Brook-Taylor-Strasse 2, 12489 Berlin (Germany)
E-mail: h.boerner@hu-berlin.de
Homepage: http://www.BoernerLab.de

[+] These authors contributed equally to this work.

Supporting information for this article can be found under: http://dx.doi.org/10.1002/anie.201601603.

on silicon substrates by micro contact printing were identified.[16]

Herein we report on the selective coating of patterns printed on cellulose paper with a commercial laser printer. This approach relies on commercial toner to print patterned surfaces. Functionalization of printed and non-printed paper regions were realized by selectively coating toner and cellulose with surface-specific 12mer peptides found by phage display. The coatings could be stabilized by photo-induced crosslinking and complex functionalities were introduced subsequently by exploiting TAD-modified dyes or functional peptides.

Phage display screening was used to select adhesive domains specific for surfaces of either paper or laser printer toner. Biopanning was executed on pre-melted original sub-micrometer toner particles to imitate the fixation step within the printing process. Moreover, pure microcrystalline cellulose was applied instead of paper to avoid selection of peptide binders to fillers, glues, or coatings. The applied phage library was composed of M13 bacteriophages with inserted randomized 12mer adhesive domains and spanned a sequential space of about 10^9 peptides. Up to four iterations of biopanning cycles on both substrates were performed and standard biopanning protocols were advanced by a negative selection step on the opposing material to enhance surface specificity (cf. Supporting Information p. S5–6). Out of the phage-pools 20 phage clones were selected after 3rd and 4th biopanning cycles for each substrate. Sequencing led to 16 cellulose binding peptides (CBP) and 4 toner-binding peptides (TBP; cf. Table 1 and Table S1). It has to be noted, that a high occurrence frequency does not necessarily correlate with increased material specificity. For a better understanding of surface-specific binding motifs, a severely larger number of sequenced phages would be required. Although the limited number of sequences does neither allow for a direct statistical evaluation nor guarantee a selection of material specific peptide-based binders, two peptides for each of the substrates where synthesized by solid-phase peptide synthesis (SPPS). For ease of analysis a *N*-terminal extension with a $(Gly)_3$ spacer and carboxyfluorescein (FAM) label was added to yield FAM-$CBP_{1\&2}$ and FAM-$TBP_{1\&2}$ (cf. Supporting Information p. S11–16). A substrate-specific selection during biopanning was confirmed by the noteworthy fact, that the selected cellulose binders exhibited strong sequence analogies to cellulose-binding motifs present in cellulose-degrading bacteria (cf. Table S2).

Table 1: Peptide sequences identified by phage display on respective substrates and occurrence frequencies in analyzed phage clones (most potent binding domains are highlighted bolt).

Sequence	Substrate	Frequency in phage display	Label
MHPNAGHGSLMR[a]	**Cellulose**	**3**	**CBP1**
TPQSFWQKGSLV[a]	Cellulose	1	CBP2
SGVYKVAYDWQH	**Toner**	**3**	**TBP1**
LPVNGDAELWHS	Toner	9	TBP2

[a] Consensus sequences with cellulose-binding domains from cellulose-degrading bacteria are underlined (for detailed information see Table S2).

To investigate the binding behavior and binding selectivity of FAM-$CBP_{1\&2}$ and FAM-$TBP_{1\&2}$ to cellulose and toner substrates, incubation/elution experiments were performed using fluorescence spectroscopy for quantification (Figure 2).

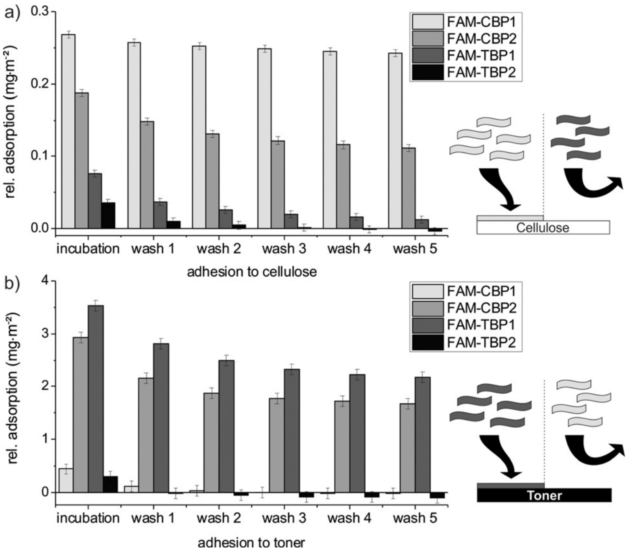

Figure 2. Incubation/elution plots of CBPs and TBPs on cellulose (a) and toner (b) showing initial adsorption, binding specificity, and final coating stability after 5 washings. Conditions: Fluorescently marked peptides (10 nmol) were dissolved in TBST buffer (0.5 mM, pH 7.5) for adsorption on cellulose, or in citrate buffer (50 mM, pH 6.5) for adsorption on toner. Peptide solutions were incubated with 50 mg of corresponding substrates for 10 min. The isolated coated substrates were washed with 1 mL of the corresponding buffer for 2 min each.

Aqueous solutions of respective peptides (10 nmol) were incubated with 50 mg of either microcrystalline cellulose or grinded toner particles. After centrifugation, the decrease of peptide concentration in the supernatant directly corresponds to the surface-adsorbed fraction (Figure 2, incubation). Subsequently, peptide elution from coated substrates was performed by five consecutive washing cycles. Measurement of the amounts of eluted peptides in washing solutions shows the stability of the resulting films (Figure 2).

Both FAM-CBPs showed under the given conditions significant adsorption onto cellulose, forming stable coatings. FAM-CBP_1 proved to be most effective, as only 10% of the initially adsorbed peptides eluted during washing, leading to a stable coating of 0.27 mg FAM-CBP_1 per gram cellulose. More importantly, however, is the cross-selectivity toward the anti-substrate. Where FAM-CBP_1 lead to minor and fully reversible adsorption to toner surfaces, FAM-CBP_2 showed practically no specificity and adheres in substantial amounts to toner. Both toner binding peptides reveal only minor and reversible adsorption onto cellulose. Nonetheless, only FAM-TBP_1 lead to a stable coating onto toner surfaces with 0.13 mg peptide per gram toner. Apparently, TBP_2 belongs to the pool of failure sequences, which are known to be found by biopanning. Those false hits exhibit low adhesive properties but can be enriched during biopanning owing to superior amplification rates of the phages in the *E. coli* host.[17] To exclude a major influence of color pigments in the toner, adsorption experiments for TBP_1 were conducted on black, yellow, magenta, and cyan blue toner (cf. Supporting Information p. S.26). Only minor differences were evident, indicating the adsorption of TBP_1 is dominated by binding to the toner polymer.

To highlight the importance of a tailored sequence originating from a selection process, two control peptides were rationally designed for cellulose and toner binding. Cationic functionalities are important for interactions with cellulose as known from, for example, poly(ethylene imine)-based retention aids for paper production.[18] Thus, Arg_{12} was tested as a cellulose binder. As an appropriate model binder for toner, Phe_6 was tested, which could interact with the poly(styrene-*co*-acrylate) matrix polymer of the toner. To provide solubility in water, both Arg_{12} and Phe_6 were conjugated to a poly(ethylene oxide) block of $M_n = 3.2 \times 10^3$ that proved in congener coatings to not significantly alter peptide–surface interactions.[19] Incubation/elution experiments showed the expected coating behavior for both model binders to their target substrates (cf. Figure S16). However, the cross-selectivity study revealed a significant adsorption of both binders to their anti-substrates. These results indicate the value of rational design strategies to address primary functions, for example, adsorption. However, the realization of complex functions, such as material specific adsorption, requires sequences that are difficult to design with the current rather limited structural insights into peptide–substrate binding.

For a better understanding of the coating behavior of the peptides, the maximum surface coverage was estimated. For that purpose, incubation/elution experiments were performed with increasing peptide concentrations until surface saturation was achieved. Taking the BET surface area of $1.1\ m^2 g^{-1}$ for cellulose into account, theoretical surface coverages could be calculated, assuming that the peptide adopts a conformation between an all-*trans* β-strand and a statistical coil (cf. Table S4). The peptide in the statistical coil covers an estimated surface area of $0.4\ nm^2$ per chain, leading to a cellulose surface coverage of approximately 40%. For the β-strand assumption, an interface of $2.1\ nm^2$ could be calculated, giving a surface coverage of about 200%. As the structure of the peptide on the cellulose surface is difficult to determine, a slightly extended coil might be expected. In solution, TBP_1 and CBP_1 adopt random coil structures, showing typical negative cotton effects at 195 nm in circular dichroism (CD) spectroscopy (cf. Supporting Information p. S24). Accurate structure determination of the adsorbed peptides, however, is not trivial and requires further investigation. Unfortunately, the grinded toner exhibits a surface area too small to be analyzed by BET in a reliable means.

Incubation/elution experiments highlighted, that CBP_1 and TBP_1 bind selectively to isolated cellulose and toner. To prove a selective coating of laser-printed patterns, where both surfaces occur next to each other, adsorption studies on printed filter paper were performed. In contrast to office paper, filter paper exhibits no coatings or fillers and prevents interference of non-specific binding to additives. Using a standard office laser printer, patterns were printed onto paper as shown in Figure 3. The applied system generally allows a resolution in the scale of approximately 100 μm, mainly limited by a decreased border sharpness of smaller patterns. For ease of analysis, TBP_1 was labeled with Rhodamine B (RhoB-TBP_1) to distinguish it from FAM-CBP_1 in fluorescence microscopy. The coating of printed patterns was performed in a two-step manner by incubating first with RhoB-TBP_1 in citrate buffer (50 mᴍ, pH 6.5) for toner coating followed by coating of cellulose with FAM-CBP_1 in TBST buffer (0.5 mᴍ, pH 7.5). Fluorescence microscopy indicated a selective coating of toner patterns during the first coating step, but a minor migration of RhoB-TBP_1 from toner to cellulose surface during the second coating step was observed (Figure S14). This result might be explained by a highly selective but weak binding of TBP_1 onto toner.

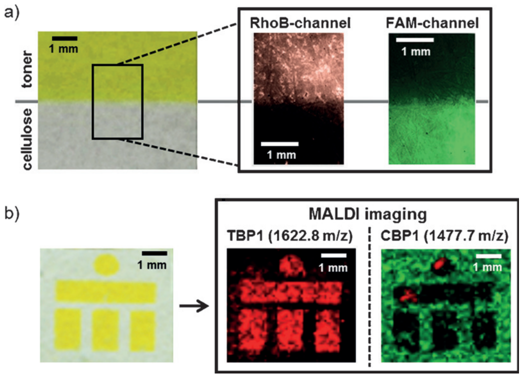

Figure 3. Analysis of the material-specific coatings of laser-printed patterns on paper. a) Fluorescence microscopy micrographs of printed paper after incubation with RhoB-TBP_1, PICUP fixation, and incubation with FAM-CBP_1 (corresponding light microscopy image (left) and fluorescence images (right)). b) MALDI imaging analysis after incubation with TBP_1 (middle) and after incubation with TBP_1, PICUP fixation, and CBP_1 incubation (right) (light microscopy image of printed pattern (left), ion flow intensity of TBP_1 (red) and CBP_1 (green)). Conditions: Printed patterns were incubated with RhoB-TBP_1/TBP_1 ($0.2\ mg\,mL^{-1}$, 50 mᴍ citrate buffer (pH 6.5), 15 min). After PICUP fixation, incubation with FAM-CBP_1/CBP_1 ($0.2\ mg\,mL^{-1}$, 0.5 mᴍ TBST buffer (pH 7.5), 10 min) followed.

To prevent this side reaction, RhoB-TBP_1/toner coatings were immobilized prior to FAM-CBP_1 incubation by applying the PICUP strategy (photo-induced cross-linking of unmodified proteins).[20] Photo-induced radical cross-linking was performed with $[Ru(bipy)_3]$ as the sensitizer by irradiation with visible light for 10 s and effectively immobilized the toner coating. Subsequent incubation with an aqueous solution of FAM-CBP_1 leads to a selective coating of the residual cellulose surfaces. Fluorescence microscopy confirmed that the stepwise coating proceeds in a controlled manner. After the cross-linking step RhoB-TBP_1 is selectively present on the printed surfaces and no fluorescence occurred on cellulose (Figure 3a). The fixation prevents RhoB-TBP_1 migration during FAM-CBP_1 incubation, as indicated by a sharp boundary between RhoB-TBP_1 coated toner and FAM-CBP_1 coated cellulose surface.

The effect of the fluorescence markers (RhoB, FAM) on the binding selectivity and coating stability of both adhesive domains was investigated. Further analysis of non-labeled TBP_1 and CBP_1 was enabled by MALDI imaging. For that purpose, coatings were prepared under conditions comparable to those described above. MALDI imaging confirmed the specific localization of both peptides on the respective substrates of a laser-printed pattern on filter paper (Figure 3b). Moreover, the absence of TBP_1 mass signals in MALDI imaging after PICUP fixation showed an effective cross-linkage of the coating.

Although a material specific adsorption of two different coatings was realized, the process remains delicate as interference with other functional segments might occur. To introduce further functionalities and functions to the specific coatings, a versatile post-coating functionalization was realized. This was implemented via chemo-selective ligation of tyrosine side-chain functionalities with 4-phenyl-1,2,4-triazoline-3,5-dione (PTAD), which has been previously described.[21] TBP_1 presents two tyrosine residues (Tyr4 and Tyr8), whereas CBP_1 is tyrosine-free. Hence, the ligation reaction can be used for selective covalent attachment of functional moieties to the toner coating on printed patterns. Figure 4 shows the introduction of PTAD functional peptide Gly_3-Rhodamine B to the selective coating of a printed toner pattern. The RhoB-labeled peptide was coupled to a 4-aminophenyl-1,2,4-triazolidine-3,5-dione (APTAD-precursor) via active ester amidation (cf. Supporting Information p. S9). After activation to the corresponding triazolindione by *N*-bromsuccinimide oxidation, ligation to the immobilized TBP_1 took place within 3 min under aqueous conditions. No side-reactions with cellulose or CBP_1 coatings were evident as indicated by fluorescence microscopy. To demonstrate the versatility of this approach, the APTAD-precursor including a Gly_3 spacer was conjugated to a model carbonate-binding peptide Pif_2 $(DDRK)_2$ originating from the aragonite binding protein Pif80 of the mollusk shell.[22] This sequence includes basic amino acids Arg/Lys that might interact with cellulose as well as cellulose-CBP_1 coatings.[18] The peptide was N-terminally extended with RhoB-GG for fluorescent detection. Subsequent functionalization of precoated, printed patterns was performed and fluorescence microscopy confirmed the highly selective modification of toner surface (cf. Supporting Information p. S23–24).

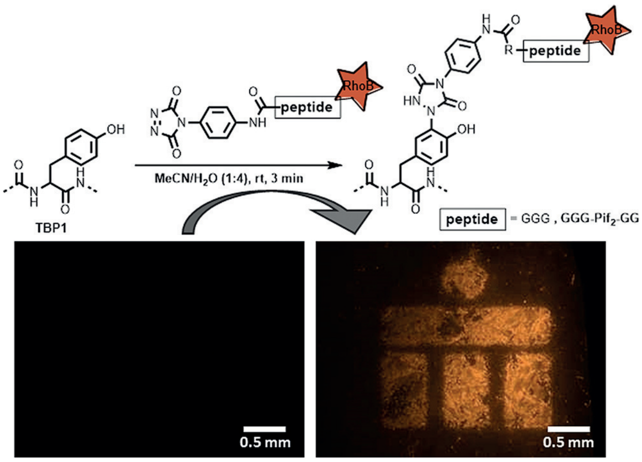

Figure 4. Triazolindione ligation of PTAD-peptide-Rhodamine B to tyrosine moieties present in the TBP_1 toner coating (top). Fluorescence microscopy before (left) and after (right) ligation demonstrated a selective functionalization of printed patterns (bottom). Conditions: Printed patterns were coated with TBP_1, crosslinked by PICUP and coated with CBP_1. PTAD-GGG-RhoB ligation in $MeCN/H_2O/DMF$ (19:76:5) for 3 min using 0.34 nmol of the active linker.

In conclusion, an advanced coating exploiting material-specific adsorption of peptides was realized, enabling the selective functionalization of laser-printed patterns and non-printed paper regions. Phage display biopanning identified 12mer peptides specifically adhering to either cellulose or toner, effectively discriminating the respective anti-substrates. Selective coating of printed patterns was shown by both fluorescence microscopy and MALDI imaging. The coatings could be fixated by photo induced radical cross-linking with a $[Ru(bipy)_3]$ sensitizer. Subsequently, introduction of complex functionalities or functional segments was demonstrated. Post-coating modification introduced triazolindione-carrying functional peptides selectively to toner coatings leaving cellulose coatings unmodified. This approach might offer easy means toward low-cost materials. Selective coating of printouts of standard office laser printers can be performed on a large scale. Subsequent modification with specific functionalities is possible on-demand within less than 5 min prior to application. Hence, we have shown a novel approach for the design of highly diverse cellulose-based functional materials.

Acknowledgments

We would like to acknowledge A. Zimathies and Dr. F. Emmerling from the Federal Institute for Materials Research and Testing (BAM) for BET measurements, Dr. S. Beck from Humboldt University of Berlin for MALDI imaging measurements as well as K. De Bruycker and Prof. Dr. F. E. Du Prez for valuable discussions. Funding was granted by the European Research Council under the European Union's 7th Framework Program (FP07–13)/ERC Starting grant "Specifically Interacting Polymer-SIP" (ERC 305064).

Keywords: biomolecule ligation · cellulose functionalization · material-specific coating · peptide functional coatings · phage display

How to cite: *Angew. Chem. Int. Ed.* **2016**, *55*, 11266–11270
Angew. Chem. **2016**, *128*, 11435–11440

---

[1] a) D. Klemm, B. Heublein, H. P. Fink, A. Bohn, *Angew. Chem. Int. Ed.* **2005**, *44*, 3358; *Angew. Chem.* **2005**, *117*, 3422; b) P. Fratzl, R. Weinkamer, *Prog. Mater. Sci.* **2007**, *52*, 1263; c) X. Qiu, S. Hu, *Materials* **2013**, *6*, 738; d) D. Klemm, F. Kramer, S. Moritz, T. Lindstrom, M. Ankerfors, D. Gray, A. Dorris, *Angew. Chem. Int. Ed.* **2011**, *50*, 5438; *Angew. Chem.* **2011**, *123*, 5550.

[2] a) A. K. Bledzki, J. Gassan, *Prog. Polym. Sci.* **1999**, *24*, 221; b) R. Derda, S. K. Y. Tang, A. Laromaine, B. Mosadegh, E. Hong, M.

Mwangi, A. Mammoto, D. E. Ingber, G. M. Whitesides, *PLoS ONE* **2011**, *6*, e18940; c) A. W. Martinez, S. T. Phillips, G. M. Whitesides, E. Carrilho, *Anal. Chem.* **2010**, *82*, 3; d) E. Morales-Narváez, H. Golmohammadi, T. Naghdi, H. Yousefi, U. Kostiv, D. Horák, N. Pourreza, A. Merkoçi, *ACS Nano* **2015**, *9*, 7296; e) S. Diekmann, G. Siegmund, A. Roecker, D. O. Klemm, *Cellulose* **2003**, *10*, 53.

[3] a) C. Wang, R. A. Venditti, K. Zhang, *Appl. Microbiol. Biotechnol.* **2015**, *99*, 5791; b) D. Rana, T. Matsuura, *Chem. Rev.* **2010**, *110*, 2448.

[4] a) X. Li, J. Tian, W. Shen, *Cellulose* **2010**, *17*, 649; b) A. Razaq, M. H. Asif, R. Kalsoom, A. F. Khan, M. S. Awan, S. Ishrat, S. M. Ramay, *J. Appl. Polym. Sci.* **2015**, *132*, 5; c) S. Kumar, S. Kumar, S. Srivastava, B. K. Yadav, S. H. Lee, J. G. Sharma, D. C. Doval, B. D. Malhotra, *Biosens. Bioelectron.* **2015**, *73*, 114; d) J.-W. Han, B. Kim, J. Li, M. Meyyappan, *J. Phys. Chem. C* **2012**, *116*, 22094; e) A. W. Martinez, S. T. Phillips, G. M. Whitesides, *Proc. Natl. Acad. Sci. USA* **2008**, *105*, 19606.

[5] a) T. Tischer, C. Rodriguez-Emmenegger, V. Trouillet, A. Welle, V. Schueler, J. O. Mueller, A. S. Goldmann, E. Brynda, C. Barner-Kowollik, *Adv. Mater.* **2014**, *26*, 4087; b) T. Tischer, A. S. Goldmann, K. Linkert, V. Trouillet, H. G. Börner, C. Barner-Kowollik, *Adv. Funct. Mater.* **2012**, *22*, 3853; c) T. Tischer, T. K. Claus, M. Bruns, V. Trouillet, K. Linkert, C. Rodriguez-Emmenegger, A. S. Goldmann, S. Perrier, H. G. Börner, C. Barner-Kowollik, *Biomacromolecules* **2013**, *14*, 4340.

[6] E. Malmström, A. Carlmark, *Polym. Chem.* **2012**, *3*, 1702.

[7] E. Tekin, P. J. Smith, U. S. Schubert, *Soft Matter* **2008**, *4*, 703.

[8] a) A. Teichler, J. Perelaer, U. S. Schubert, *J. Mater. Chem. C* **2013**, *1*, 1910; b) E. Carrilho, A. W. Martinez, G. M. Whitesides, *Anal. Chem.* **2009**, *81*, 7091; c) D. Hohnholz, H. Okuzaki, A. G. MacDiarmid, *Adv. Funct. Mater.* **2005**, *15*, 51; d) N. Komuro, S. Takaki, K. Suzuki, D. Citterio, *Anal. Bioanal. Chem.* **2013**, *405*, 5785; e) B. J. de Gans, P. C. Duineveld, U. S. Schubert, *Adv. Mater.* **2004**, *16*, 203.

[9] a) F. Baneyx, D. T. Schwartz, *Curr. Opin. Biotechnol.* **2007**, *18*, 312; b) H. G. Börner, *Macromol. Rapid Commun.* **2011**, *32*, 115; c) Q. Wei, K. Achazi, H. Liebe, A. Schulz, P.-L. M. Noeske, I. Grunwald, R. Haag, *Angew. Chem. Int. Ed.* **2014**, *53*, 11650; *Angew. Chem.* **2014**, *126*, 11834; d) P. Wilke, N. Helfricht, A. Mark, G. Papastavrou, D. Faivre, G. H. Börner, *J. Am. Chem. Soc.* **2014**, *136*, 12667; e) F. Hanßke, E. Kemnitz, G. H. Börner, *Small* **2015**, *11*, 4303; f) T. Schwemmer, J. Baumgartner, D. Faivre, H. G. Börner, *J. Am. Chem. Soc.* **2012**, *134*, 2385; g) J.-F. Lutz, Z. Zarafshani, *Adv. Drug Delivery Rev.* **2008**, *60*, 958; h) A. K. Muszanska, H. J. Busscher, A. Herrmann, H. C. van der Mei, W. Norde, *Biomaterials* **2011**, *32*, 6333; i) T. Sawada, H. Mihara, T. Serizawa, *Chem. Rec.* **2013**, *13*, 172; j) T. Paulöhrl, A. Welle, M. Bruns, K. Linkert, H. G. Börner, M. Bastmeyer, G. Delaittre, C. Barner-Kowollik, *Angew. Chem. Int. Ed.* **2013**, *52*, 9714; *Angew. Chem.* **2013**, *125*, 9896; k) J. K. Berg, T. Jordan, Y. Binder, H. G. Börner, D. Gebauer, *J. Am. Chem. Soc.* **2013**, *135*, 12512; l) K. M. Marks, M. Rosinov, G. P. Nolan, *Chem. Biol.* **2004**, *11*, 347.

[10] A. B. Sanghvi, K. P. H. Miller, A. M. Belcher, C. E. Schmidt, *Nat. Mater.* **2005**, *4*, 496.

[11] T. Serizawa, H. Matsuno, T. Sawada, *J. Mater. Chem.* **2011**, *21*, 10252.

[12] S. Ju, K.-Y. Lee, S.-J. Min, Y. K. Yoo, K. S. Hwang, S. K. Kim, H. Yi, *Sci. Rep.* **2015**, *5*, 1.

[13] M.-K. Liang, O. Deschaume, S. V. Patwardhan, C. C. Perry, *J. Mater. Chem.* **2011**, *21*, 80.

[14] R. R. Naik, S. J. Stringer, G. Agarwal, S. E. Jones, M. O. Stone, *Nat. Mater.* **2002**, *1*, 169.

[15] C.-Y. Chiu, Y. Li, L. Ruan, X. Ye, C. B. Murray, Y. Huang, *Nat. Chem.* **2011**, *3*, 393.

[16] Y. Cui, A. Pattabiraman, B. Lisko, S. C. Collins, M. C. McAlpine, *J. Am. Chem. Soc.* **2010**, *132*, 1204.

[17] M. Vodnik, U. Zager, B. Strukelj, M. Lunder, *Molecules* **2011**, *16*, 790.

[18] M. A. Hubbe, H. Nanko, M. R. McNeal, *BioResources* **2009**, *4*, 850.

[19] P. Wilke, G. H. Börner, *Eur. Polym. J.* **2015**, *62*, 374.

[20] G. W. Preston, A. J. Wilson, *Chem. Soc. Rev.* **2013**, *42*, 3289.

[21] a) H. Ban, J. Gavrilyuk, C. F. Barbas III, *J. Am. Chem. Soc.* **2010**, *132*, 1523; b) S. Billiet, K. De Bruycker, F. Driessen, H. Goossens, V. Van Speybroeck, J. M. Winne, F. E. Du Prez, *Nat. Chem.* **2014**, *6*, 815.

[22] M. Suzuki, K. Saruwatari, T. Kogure, Y. Yamamoto, T. Nishimura, T. Kato, H. Nagasawa, *Science* **2009**, *325*, 1388.

Received: February 15, 2016